Journal of Materials Science and Engineering B 10 (1-2) (2020) 18-33
doi: 10.17265/2161-6221/2020.1-2.003

BOD Composite as a New Eco-Friendly Corrosion Inhibitor

A.M. Eldesoky[1,5], A. Attia[2,6], Omayma E. Ahmed[3] and M. Abo-Elsoud[4]

1. Engineering Chemistry Department, High Institute of Engineering & Technology, New Damietta 34517, Egypt

2. Chemistry Department, Mansoura University, Faculty of Science, Mansoura 35516, Egypt

3. Evaluation and Analytical Department Egyptian Petroleum Research Institute, Nasr City, Cairo 11717, Egypt

4. Physics Department, Umm Al-Qura University, Al-Qunfudhah University College, Al-Qunfudhah 21912, Saudi Arabia

5. Chemistry Department, Umm Al-Qura University, Al-Qunfudhah University College, Al-Qunfudhah 21912, Saudi Arabia

6. Chemistry Department, Najran University, Faculty of Science and Arts, Najran 21497, Saudi Arabia

Abstract: BOD composite, (E)-4-(2-(benzo[d]oxazol-2-yl) vinyl)-N,N-dimethylaniline is a new eco-friendly corrosion inhibitor versus P355 Carbon Steel (Cs). BOD was examined in 1.0 N HCl corrosive solution utilizing TP, EIS and EFM tests. EIS curves show that adsorption of BOD increases the transfer resistance and decrease the capacitance of interface metal/solution. Molecular docking was utilized to predict the binding between BOD composite with the receptor of 3tt8-hormone of crystal structure analysis of Cu Human Insulin Derivative. The morphology of inhibited P355 Cs was analyzed by checking electron magnifying instrument innovation with energy dispersive X-beam spectroscopy (SEM–EDX).

Keywords: BOD, eco-friendly, P355 Cs, SEM, EDX, molecular docking.

1. Introduction

Over the previous decades, the passivation and corrosion performance of the steel in existing have been studied [1, 2]. In the typical environment, numerous research has attentive on the electrochemical performance of traditional Cs, austenitic or duplex stainless steel (SS) kinds such as Q235 [3], 304 [4], 316 [5] or 2205 [6, 7] SS [8]. In the field of nuclear manufacturing, the steel strengthening is showing to concrete pore solution over the pH range 12 to 14 in the anoxic environs even for hundreds of years [9]. In these great alkaline environs, an inhibitive passive film will be designed spontaneously and maintained on the surface of the P355 Cs [10, 11]. The conformation of the existing pore solution has great influence on the protection of the Cs [12, 13]. However, till now, few preceding works have attentive on the electrochemical performance of the *P*355 Cs in "high alkaline" and "super-anoxic" environment [14]. We trust that the analysis of the passive manner in saturated $Ca(OH)_2$ solution (SCS) with altered pH by appending of NaOH, which was utilized as simulated concrete pore solution (SCPS), will give to an enhanced understanding of the corrosion manner of the Cs in concrete.

Since the accepted rate of corrosion of the steel in focused is very low, very long time is wanted to estimate the corrosion manner which is impractical to attain based on research laboratory experiments [15]. Therefore, electrochemical test is often utilized for rapid estimation of steel corrosion [16, 17]. Till currently, the electrochemical and protected films of P355 Cs joining in alkaline high (pH > 12.5) and anoxic environs at more polarization had negative (-1.0 V-0 V) potential are scarcely examined [18-20]. So, it is very worth travelling the structure and goods of the hindrance film obtain on P355 Cs in this condition [21-23].

Corresponding author: M. Abo-Elsoud, doctor, professor, research field: experimental physics.

The main scope of our work is to show that, the electrochemical habit of BOD as a new eco-friendly corrosion protection for P355 Cs hold 1.0 N corrosive solution is obtain by tafel polarization (Tp), (EIS) AC impedance spectroscopy and (EFM) electrochemical frequency modulation method. A few quantum-chemistry measurements have been gotten in order to record the inhibition and hindrance to the molecular properties of the composite [24, 25]. Molecular docking was utilized to predict the binding between BOD composite with the receptor of 3tt8-hormone of crystal structure analysis of Cu Human Insulin Derivative. SEM and EDX investigations of the P355 Cs in 1.0 N corrosive solution surface were examined.

2. Experimental Section

2.1 Measurements

This paper mimics the real docking procedure in which the ligand–protein pair-wise interface energies are calculated utilizing Docking Server [26]. Docking measurements were carried out on BOD composite protein model. Essential hydrogen atoms, Koll- man united atom type charges, and solvation parameters were additional with the aid of Auto-Dock tools [27]. Affinity (grid) maps of 20 × 20 × 20 A° grid points and 0.375 A° area were produced utilizing the Auto grid program [28].

2.2 Material and Medium

P355 Cs was utilized for the measurement of corrosion. It's percent composition is given in Table 1, the rest iron. The corrosion dose (1.0 N corrosive solution) (37% analytical grade) was ready by hydrochloric acid dilution with water double distilled. BOD composite utilized for this paper, whose structure was given in Table 2 [29].

2.3 Methods

2.3.1 Electrochemical Method

The electrochemical techniques have been performed utilizing 750 software for calculations. The utilized electrical circuit contains of three electrodes (SCE reference electrode, Pt auxiliary electrode and Cs electrode). 1 cm^2 of the Cs electrode is prepared. The pre-dipping oxide film was reduced by given a time period of about 20 minutes for open circuit potential (OCP). All electrochemical studies were performed at 25 ± 1 °C. *Tp* is a useful method because they give more information about the corrosion mechanism and the factors affecting the corrosion procedure and inhibition behavior of the BOD. This is done by measuring the potential-current characteristics of the metal/solution system. In *TP* measurements, electrode potential from –50 to 50 V was applied at scanning rate 1 mVs^{-1}.

(EFM) and (EIS) tests were gain by utilized the same tests as before with a Gamry framework system depend on ESA400. EIS tests were ready in a range of frequency of 100 kHz to 10 MHz with amplitude of 5 mV peak-to-peak. EFM had done utilized 2 frequencies 2 and 5 Hz. The frequency base was 1 Hz.

Table 1 Chemical conformation of the P355 Cs.

Mo	Cr	Ni	Cu	Si	S	P	Mn	C
0.009	0.082	0.05	0.043	0.324	0.0005	0.005	0.98	0.15
N	H	B	Co	Ti	V	Zr	Nb	Al
0.034	0.006	0.001	0.001	0.001	0.005	0.0001	1.95	0.034

Table 2 Chemical structure, name, molecular weight and molecular formula of inhibitor.

Structure	Name	Mol. Wt./M. formula
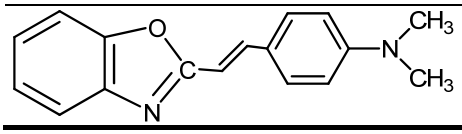	BOD	264.32/$C_{17}H_{16}N_2O$

2.3.2 SEM-EDX Tests

The surface of P355 Cs was obtained by keeping the coins for 3 days putted in 1.0 N corrosive solution with and lack of perfect dose of BOD composite, after abraded mechanically utilized unlike papers emery up to grit size 1,200. Then, after this time dipping, the samples were lotion gently with distilled water, carefully dried and mounted into the spectrometer attendance of further treatment. The surface of P355 Cs was tested utilized an X-ray diffractometer Philips (pw-1390) with Cu-tube (CuK-α, λ = 1.54051 A°), (SEM, JOEL, JSM-T20, Japan).

2.3.3. Theoretical Study

Quantum chemical measurements have been utilized Accelrys (Material Studio Version 4.4).

3. Results and Discussion

3.1. Tp Tests

Tp curves without and with different BOD concentrations for P355 Cs dissolution in corrosive solution were illustrated in Fig. 1. The variation of corrosion potential E_{corr} and, i_{corr}, β_a, β_c, CR, θ and $\%IE_P$ with BOD concentration were given in Table 3 Experimental results indicate that i_{corr} is significantly decreases with increasing BOD concentration. Both the anodic and cathodic curves were affected by the presence of BOD, i.e. BOD limited both the anodic and cathodic reactions (mixed type inhibitor). The almost unchanged Tafel slopes indicate that BOD acts by just blocking the metal surface reaction sites without changing the mechanisms of the anodic and cathodic reaction.

The $\%IE_P$ and θ from Tp measurements, were determined by applying the following equation:

$$\%IE_P = \theta \times 100 = [1 - (i^{\circ}_{corr}/i_{corr}] \times 100 \quad (1)$$

i°_{corr} and i_{corr} are the current corrosion densities lack and attendance of solution inhibitor, sequentially.

The adding of BOD to 1.0 N HCl Makes E_{corr} slightly shifted, which suggests that BOD can be considered as a mixed type inhibitor [30, 31] and also, this addition does not change the $(\beta_a \; and \; \beta_c)$ remarkably, which designates that the liberated hydrogen mechanism and the dissolution process of $P355 \; Cs$ are not affected.

3.2. EIS Tests

Fig. 2 was given Nyquist (a) and Bode (b) curves for the corrosion behavior of P355 Cs in 1.0 M HCl with and without various doses of BOD after 30 min of immersion. Impedance spectra showed one time constant related to a single capacitive semi-circles, which indicated that the corrosion procedure was mostly controlled by charge transfer [32-39]. The

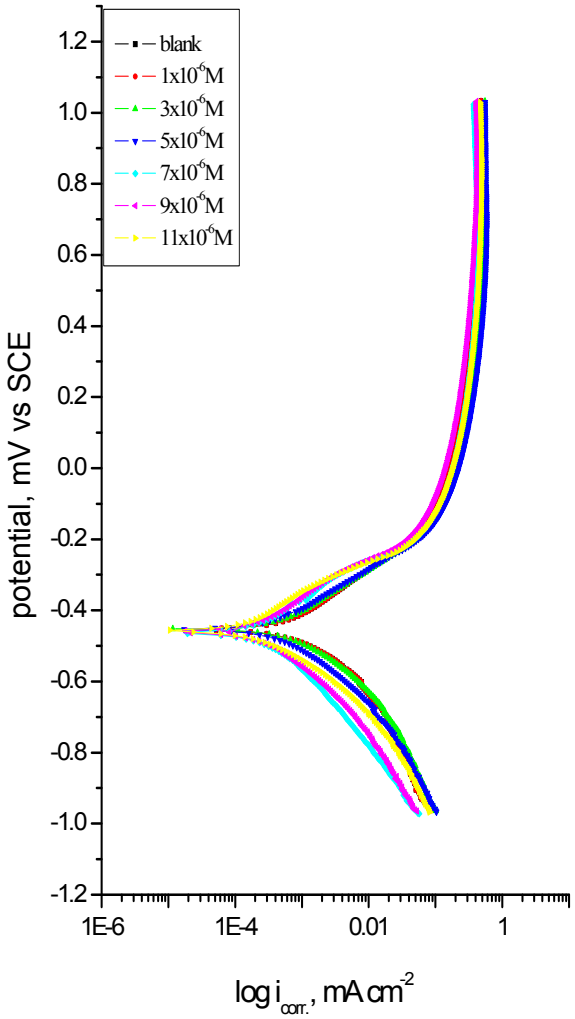

Fig. 1 ***Tp*** **curves without and with different BOD concentrations for P355 Cs dissolution in corrosive solution at 25 ± 0.1 °C.**

Table 3 Effect of BOD concentration on E_{corr}, i_{corr}, β_a, β_c, CR, θ, $\%IE_p$.

Composite	Conc., *M.*	-E_{corr} (*mV vs.SCE*)	$i_{corr}\times10^{-5}$ (μAcm^{-2})	$\beta_a\times10^{-3}$ (mV dec^{-1})	$\beta_c\times10^{-3}$ (mV dec^{-1})	θ	$\%IE_p$
	Blank	456	78.2	138.9	162.4	----	----
BOD	$1x10^{-6}$	476	69.2	136.4	163.4	0.115	11.5
	$3x10^{-6}$	454	40.4	108.5	118.3	0.483	48.3
	$5\ x10^{-6}$	456	39.2	131.7	126.9	0.498	49.8
	$7x10^{-6}$	455	33.1	201.2	173.7	0.576	57.6
	$9x10^{-6}$	476	26.5	168.3	162.4	0.661	66.1
	$11x10^{-6}$	461	17.9	109.1	151.8	0.771	77.1

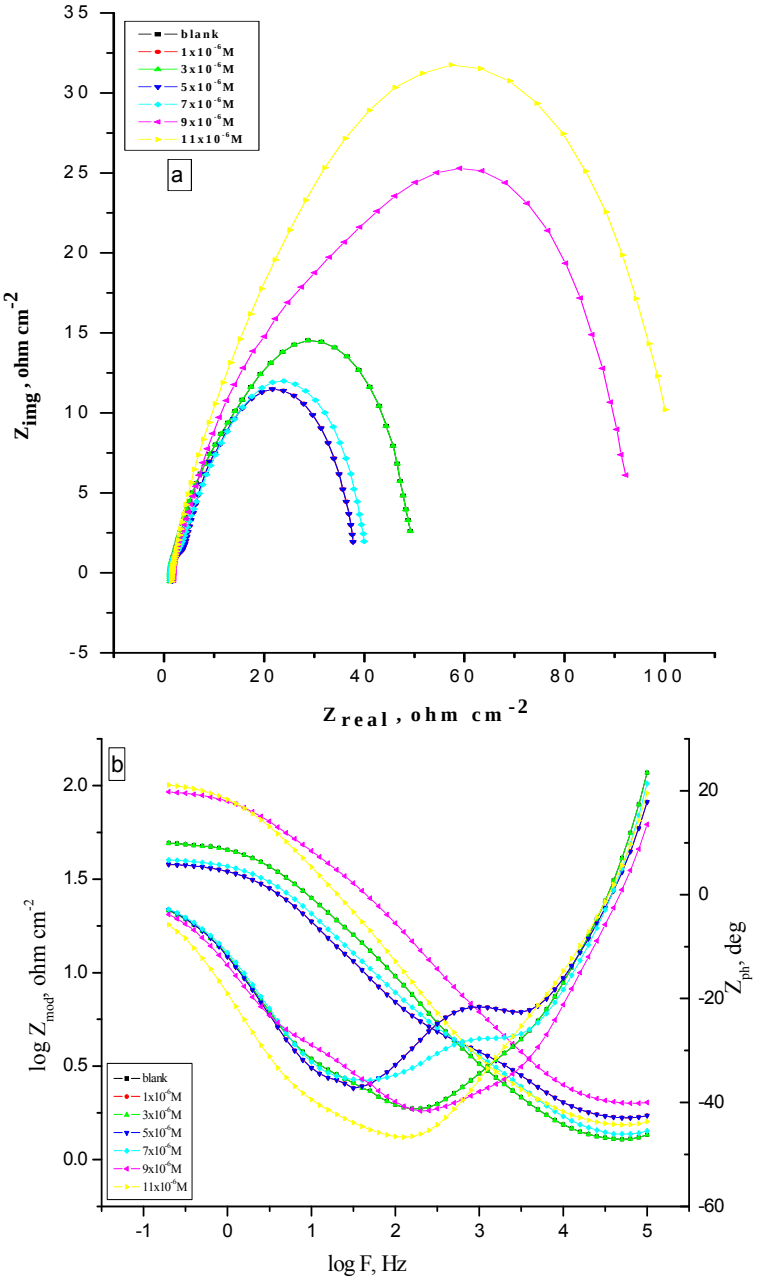

Fig. 2 The Nyquist (a) and Bode (b) diagrams for P355 Cs in 1.0 N HCl before and after adding various doses of BOD at 25 ± 0.1 °C.

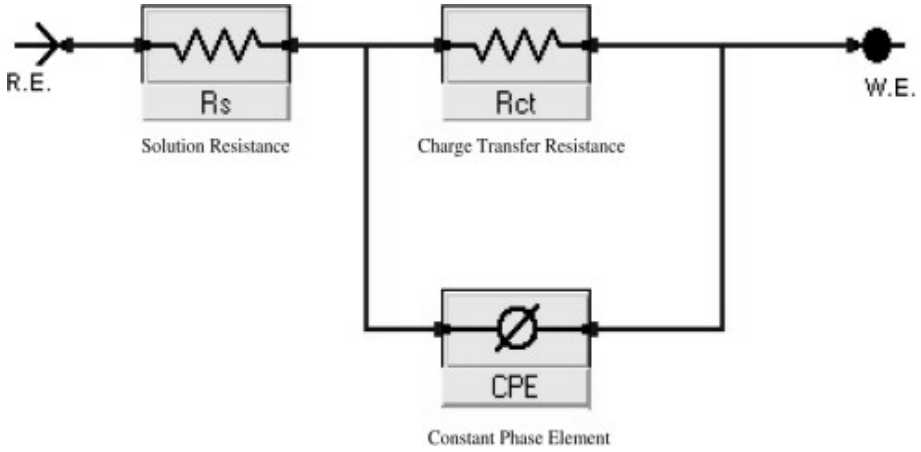

Fig. 3 Electrical equivalent circuit used to fit the EIS.

Table 4 EIS parameters for P355 Cs in 1.0 N HCl before and after adding different doses of BOD at 25 ± 0.1 °C.

Composite	Conc., *M.*	$R_S \times 10^{-3}$ (Ω cm^2)	$Y_o \times 10^{-6}$	$n \times 10^{-3}$	R_{ct} (Ω cm^2)	$C_{dl} \times 10^{-4}$ (μFcm^{-2})	θ	*IE*
	Blank	1.347	0.267	878.1	19.72	6.313	----	----
BOD	1×10^{-6}	1.831	0.302	871.9	22.91	2.751	0.139	13.9
	3×10^{-6}	1.459	0.304	865.9	23.66	2.047	0.166	16.6
	5×10^{-6}	1.793	0.213	874.7	28.92	1.986	0.318	31.8
	7×10^{-6}	1.247	3.521	551.2	46.11	1.856	0.572	57.2
	9×10^{-6}	1.705	1.211	590.1	97.01	1.858	0.796	79.6
	11×10^{-6}	1.451	1.489	642.1	111.04	1.394	0.822	82.2

obtained curves are very similar to each other, indicating that the mechanism of corrosion is not different after appending of BOD [40]. The diameter of Nyquist diagrams rises on rising of the BOD dose due to the creation of adsorbed layer of BOD on surface of P355 Cs. Fig. 3 showed the fitting equivalent circuit for EIS data, which is consisted of solution resistance (R_s), resistance charge-transfer (R_{ct}), and a CPE instead of a pure capacitor signifies the interfacial capacitance. The data of the capacitance double layer (C_{dl}) can be given from equation 2 [41]:

$$C_{dl} = Y_o \omega^{n-1} / \sin [n(\pi/2) \quad (2)$$

where $Y_o = CPE$ magnitude, $\omega = 2\pi f_{max,}$ f_{max} is the imaginary frequency at which the component of the impedance is maximal.

Table 4 represents the data of R_s, R_{ct}, $C_{dl,}$ and %*IE*. The R_{ct} is a diameter of great frequency loop, which enhancement with rising of BOD dose. While the values of C_{dl} decreases due to water replacement by extract molecules making a inhibitive layer at the P355 Cs [42-44].

The obtained $(\%\, IE)$ and (θ) of the ASE was elaborated from next (3) [45]:

$$\%IE_{EIS} = [1 - (R_{ct}^{\circ}/R_{ct}) \times 100 \quad (3)$$

Where R_{ct}° and R_{ct} are the resistance data before and after adding ASE, respectively.

3.3. EFM Test

Electrochemical frequency modulation is AC technique, but it immediately gives corrosion current values without previous knowledge of Tafel constants. Fig. 4 shows the EFM spectra for P355 Cs in 1 N HCl without and with different concentrations of BOD at 25 ^{o}C.

The parameters from EFM measurements (i_{corr}, β_a, β_c, *CF*-2, *CF*-3, *CR*, θ and %*IE*) were listed in Table 5. It is observed from the data that, the value of i_{corr} decreases by increasing BOD concentration and %*IE* increases. If the causality factors are approximately equal to 2.0 and 3.0 for CF-2, CF-3, respectively, this indicates the presence of a causal relationship between the perturbation signal and the response signal, and

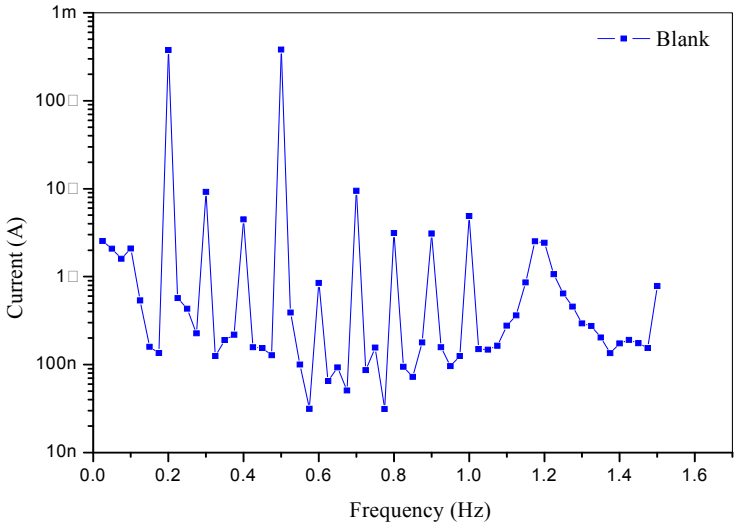
Blank
Current (A)
1m
100□
10□
1□
100n
10n
0.0
0.2
0.4
0.6
0.8
1.0
1.2
1.4
1.6
Frequency (Hz)

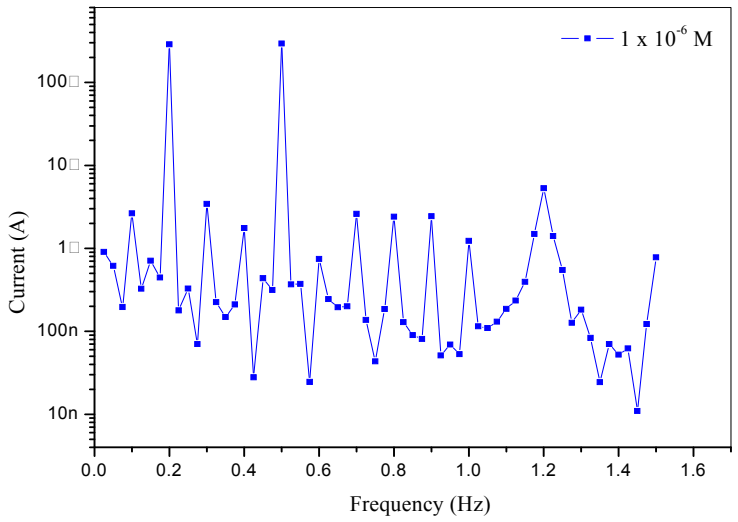
1 x 10-6 M
Current (A)
100□
10□
1□
100n
10n
0.0
0.2
0.4
0.6
0.8
1.0
1.2
1.4
1.6
Frequency (Hz)

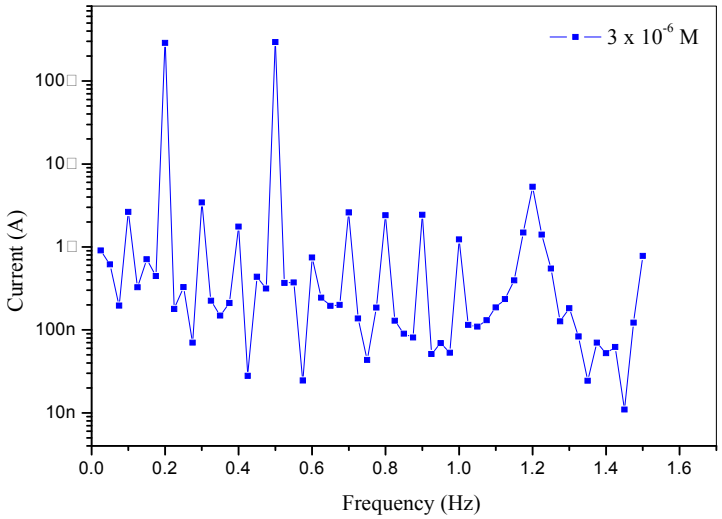
3 x 10-6 M
Current (A)
100□
10□
1□
100n
10n
0.0
0.2
0.4
0.6
0.8
1.0
1.2
1.4
1.6
Frequency (Hz)

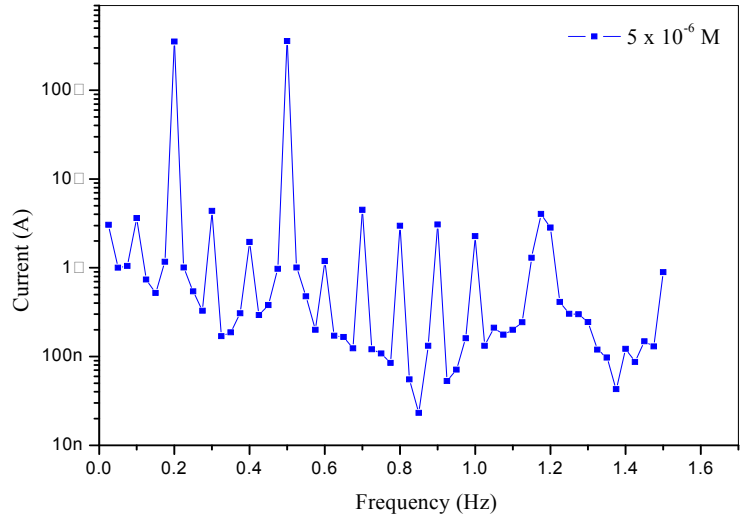
5 x 10-6 M
Current (A)
100
10
1
100n
10n
0.0
0.2
0.4
0.6
0.8
1.0
1.2
1.4
1.6
Frequency (Hz)

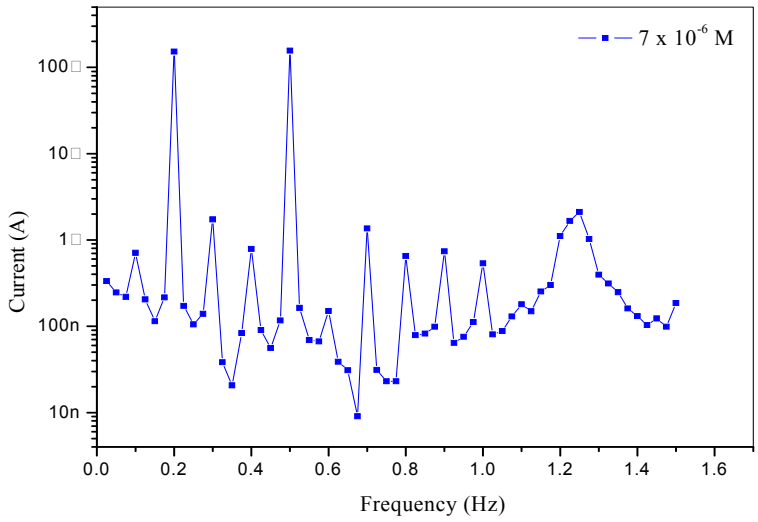
7 x 10-6 M
Current (A)
100
10
1
100n
10n
0.0
0.2
0.4
0.6
0.8
1.0
1.2
1.4
1.6
Frequency (Hz)

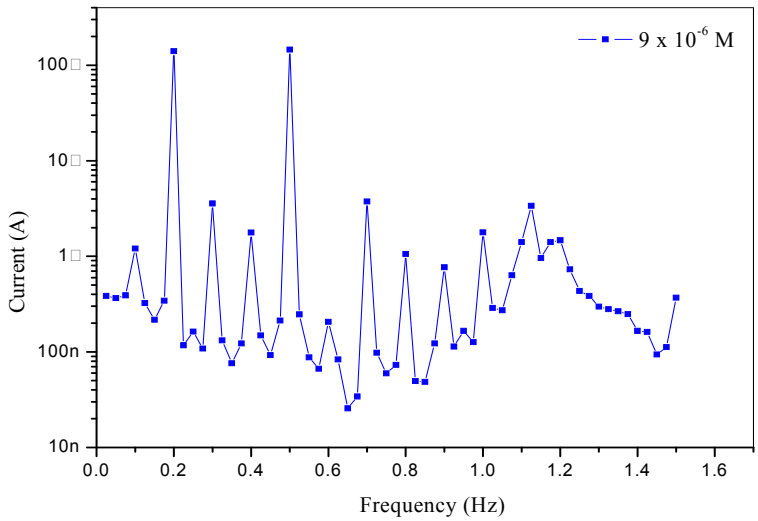
9 x 10-6 M
Current (A)
100
10
1
100n
10n
0.0
0.2
0.4
0.6
0.8
1.0
1.2
1.4
1.6
Frequency (Hz)

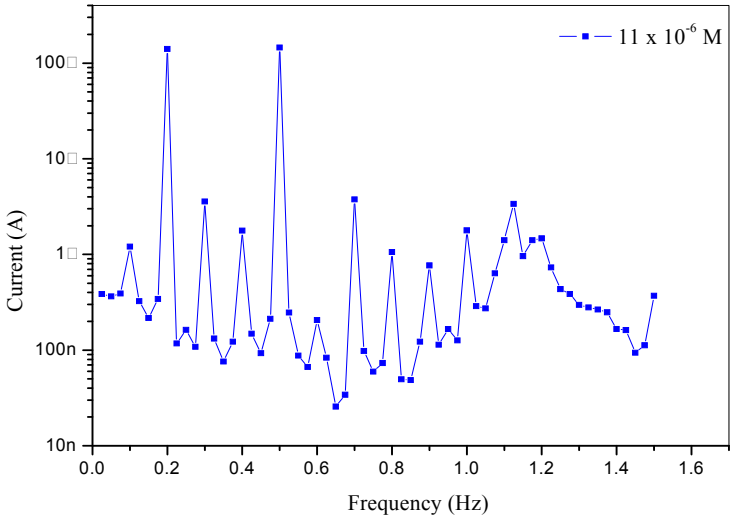

Fig. 4 EFM spectra for *P*355 CS in 1.0 N HCl before and after adding various.

Table 5 EFM parameters for P355 Cs before and after adding various doses of BOD in 1.0 N HCl at 25 ± 0.1 °C.

Composite	Conc., *M.*	i_{corr} ($\mu A cm^{-2}$)	$\beta_a \times 10^{-3}$ (mV dec^{-1})	$\beta_c \times 10^{-3}$ (mV dec^{-1})	*CF-2*	*CF-3*	θ	*%IE*
	Blank	821.5	126.8	158.4	1.98	3.06	-----	------
BOD	1×10^{-6}	666.3	118.9	130.4	2.02	3.01	0.188	18.8
	3×10^{-6}	488.2	107.5	123.2	2.03	3.07	0.405	40.5
	5×10^{-6}	471.6	107.9	113.6	2.01	3.02	0.425	42.5
	7×10^{-6}	360.4	111.2	161.2	2.01	2.89	0.561	56.1
	9×10^{-6}	266.3	118.7	149.4	2.01	3.03	0.675	67.5
	11×10^{-6}	253.2	117.8	140.6	1.96	2.98	0.691	69.1

the results are considered to be trusted [46]. Deviation of CF-2 and CF-3 values from ideality may be because the perturbation amplitude was overly small, or the frequency spectrum resolution is not sufficiently high, or the inhibitor is not working very well [47].

The IE_{EFM} % improve by rising the BOD doses and was obtain as follows:

$$\%IE_{EFM} = [1 - (i_{corr}/i^{\circ}_{corr}) \times 100 \qquad (4)$$

where i°_{corr} and i_{corr} are current densities before and after adding BOD, correspondingly.

3.4. SEM Tests

Fig. 5 demonstrates the morphology of the surface of P355 *CS* coins polished before exposure to the corrosive solution, SEM image of the CS after dipping in HCl for 3 day. The micrographs displayed an extended etching contain green and dark areas with damaged highly [48, 49].

Fig. 5 (with 11×10^{-6} M of BOD) is clear that BOD provided best protection at the surface of the P355 Cs metal as it forms a inhibitive film on the P355 Cs surface.

3.5 EDS Test

The EDS spectra were utilized to measure the elements found on the surface of P355 Cs after 3 days of covered in the lack and attendance of 1.0 N corrosive solution. Fig. 6 gives the EDS result measured on the composition of P355 Cs only without the acid and inhibitor modified. The EDS record that only oxygen and iron were observed, which given that the passive film found with only Fe_2O_3.

The EDS tests of P355 Cs in 1.0 N corrosive solution only and with of 11×10^{-6} M of BOD composite portrays in Fig. 6. The spectra give additional lines,

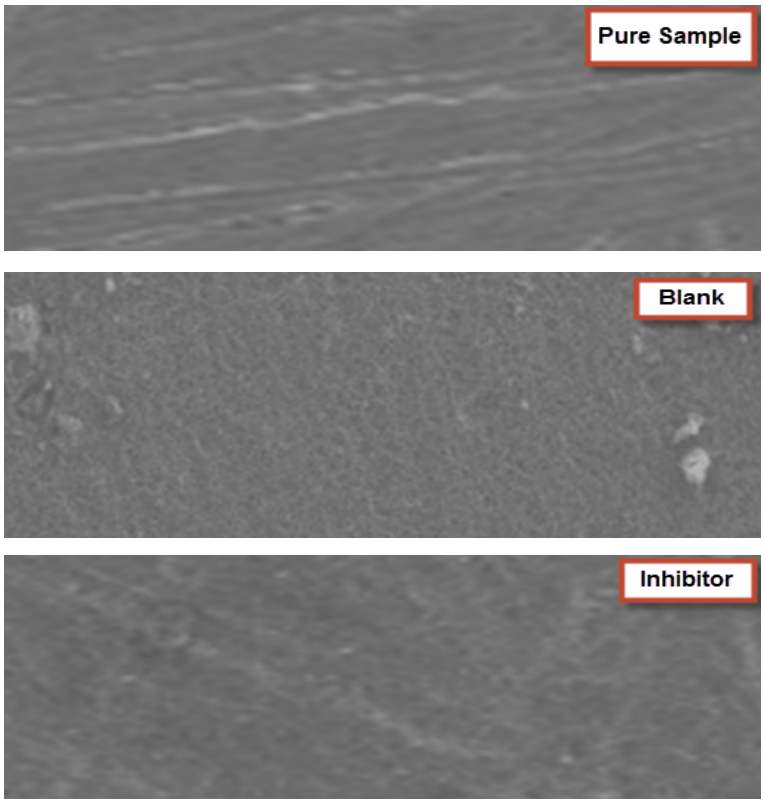

Fig. 5 SEM of P355 Cs in 1.0N corrosive solution after dipping for 3 days nonexistence inhibitor and existence of 11 × 10^{-6} *M* of BOD.

lead to the presence of C (the carbon atoms of BOD compound). These values give that the O and C atoms covered surface. The elemental observed is record in Table 6.

3.6. Quantum Chemical Measurements

The Mulliken charge and molecular orbital curve of BOD composite are given in Fig. 7. Theoretical measurements were found for only the forms of neutral, in order to obtain further insight into the results of experimental. Data of quantum chemical lead to energies of energy gap (ΔE) and (E_{HOMO}) energy of highest occupied molecular orbitals and (E_{LUMO}) are measured and record in Table 7. The increase or lower negative E_{HOMO} is inhibitor associated, the higher the trend of offering electrons to unoccupied d orbital of P355 Cs, and the improvement the corrosion protection. Due to the decrease of E_{LUMO}, the acceptance of electrons is plain from P355 Cs surface [50, 51].

Apparently, good corrosion protection is usually those BOD composites who are not only offer electrons to unoccupied orbital of the alloy, but also free electrons established from the metal [52]. It can be seen that all measurement of quantum parameters checking these results from experimental.

3.7 Molecular Docking

The docking research displayed a favorable interface among BOD composite and the receptor of 3tt8-hormone of crystal structure investigation of Cu Human Insulin Derivative. "The calculated energy is listed in Table 8 and Fig. 8. According to the results obtained in this study, HB plot curve indicated that, the BOD composite binds to the proteins hydrogen bond and decomposed interactions energies in kcal/mol were existed between the BOD composite with 3tt8 receptor as shown in Fig. 9. The calculated efficiency is favorable where K_i values estimated by Auto Dock were compared with experimental K_i

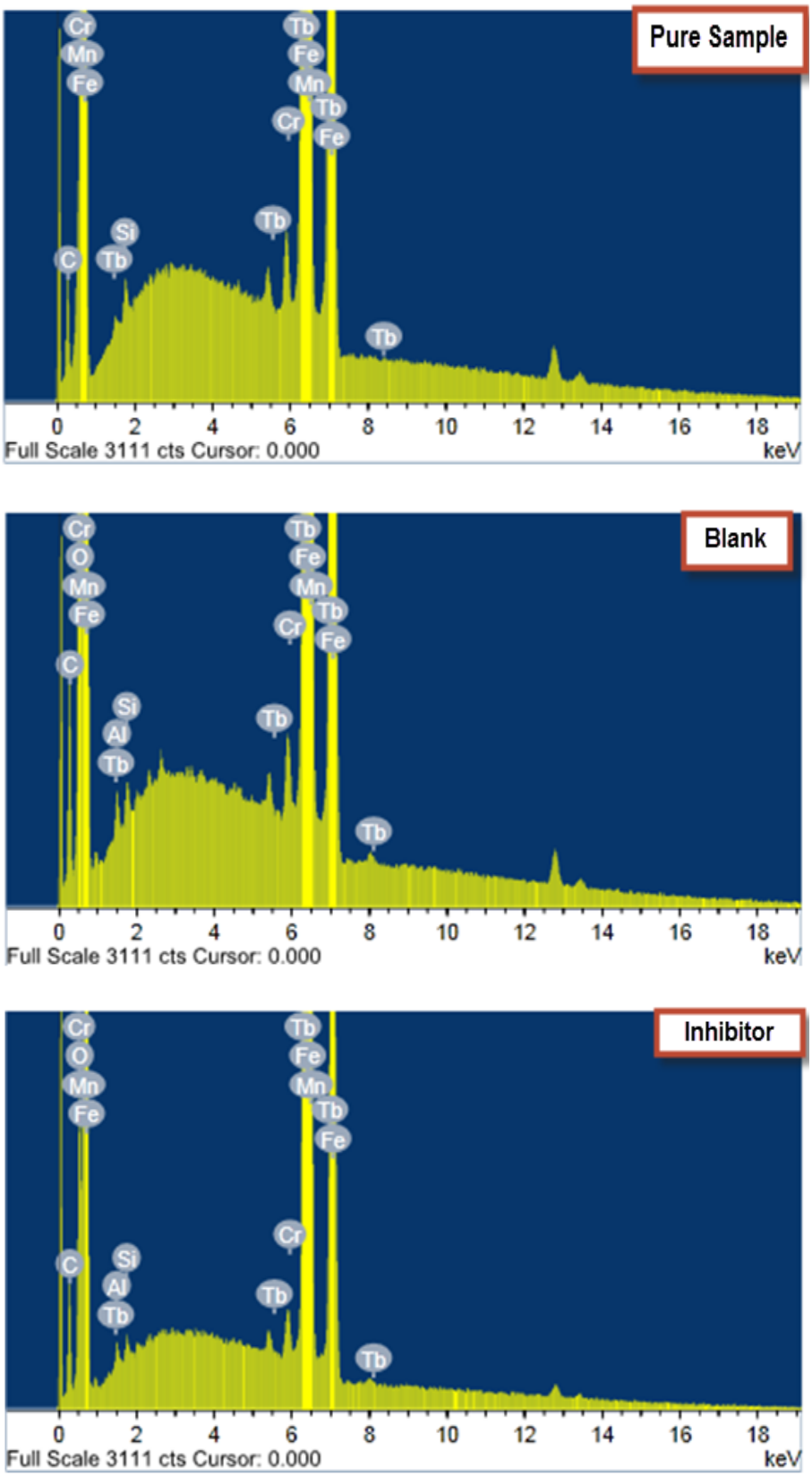

Fig. 6 ***EDS*** **study of P355 Cs in 1.0 N corrosive solution after dipping for 3 days nonexistence inhibitor and existence of 11 × 10^{-6}** ***M*** **of BOD compound.**

Table 6 Mass % of P355 Cs after 3 days in HCl lack and attendance of the optimum dose of the studied BOD compound.

(Mass %)	C	O	Al	Si	Cr	Mn	Fe	Tb
Pure Sample	6.79	---	0.28	0.25	0.26	0.49	89.60	2.33
Blank	8.51	14.99	0.26	0.24	0.13	0.41	73.37	2.09
Inhibitor	13.23	6.77	0.27	0.23	0.19	0.42	76.58	2.31

Table 7 The quantum chemical properties for examined BOD compound.

Properties	Inhibitor
$-E_{HOMO}$ (eV)	0.2767
$-E_{LUMO}$ (eV)	0.1555
ΔE (eV)	0.1211
η (eV)	0.0605
σ $(eV)^{-1}$	16.5111
$-Pi$ $(a.u)$	0.2161
X (eV)	0.2161
S $(eV)^{-1}$	8.2555
ω (a.u)	0.3857
ΔN_{max}	3.5689

Inhibitor	BOD
HOMO	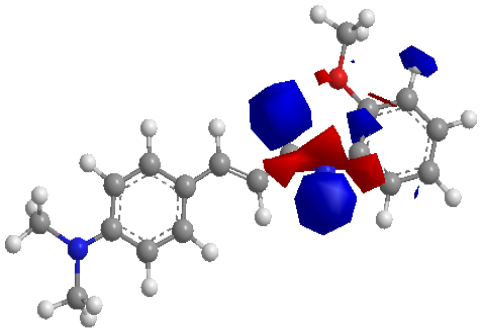
LUMO	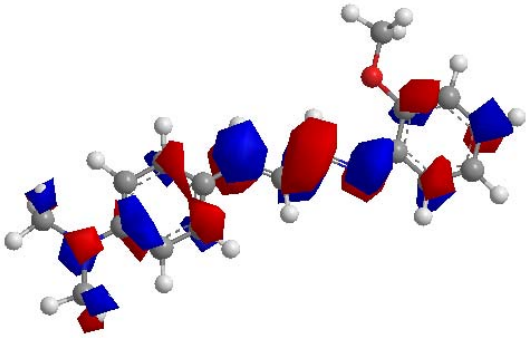
Molecular Structure	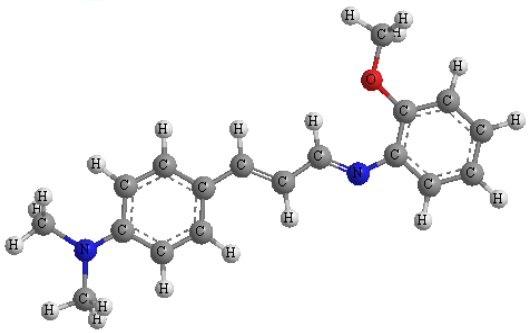

Fig. 7 Molecular orbital plots of investigated BOD compound.

Compound	(A)	(B)
BOD	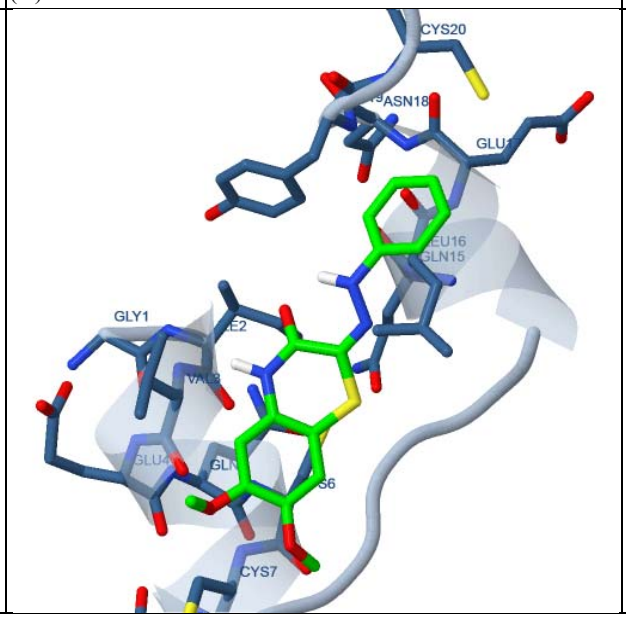	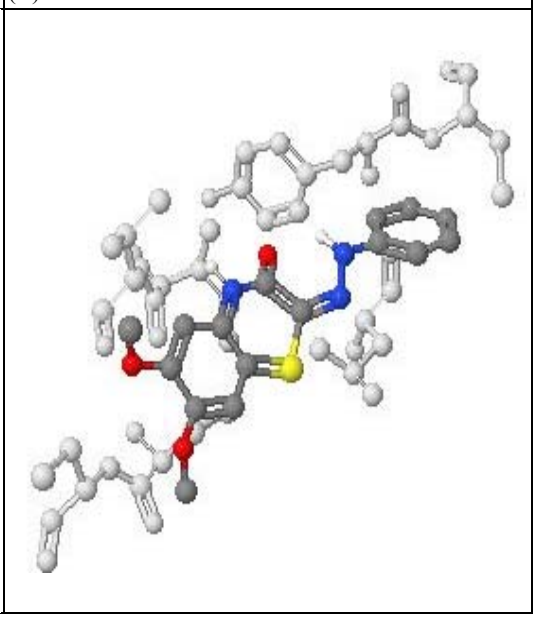

Fig. 8 BOD composite (green in (A) and gray in (B)) in interaction with 3tt8 receptor. (For interpretation of the references to color in this figure legend, the reader is referred to the web version of this article).

Table 8 Energy data gotten in docking tests of BOD composite with 3tt8 receptor.

Compound	Est. free energy of binding (kcal/mol)	Est. inhibition constant (K_i) (μM)	vdW+ bond+ desolve energy (kcal/mol)	Electrostatic energy (kcal/mol)	Total intercooled energy (kcal/mol)	Interact surface
BOD	-4.66	383.22	-5.41	-0.01	-5.41	533.617

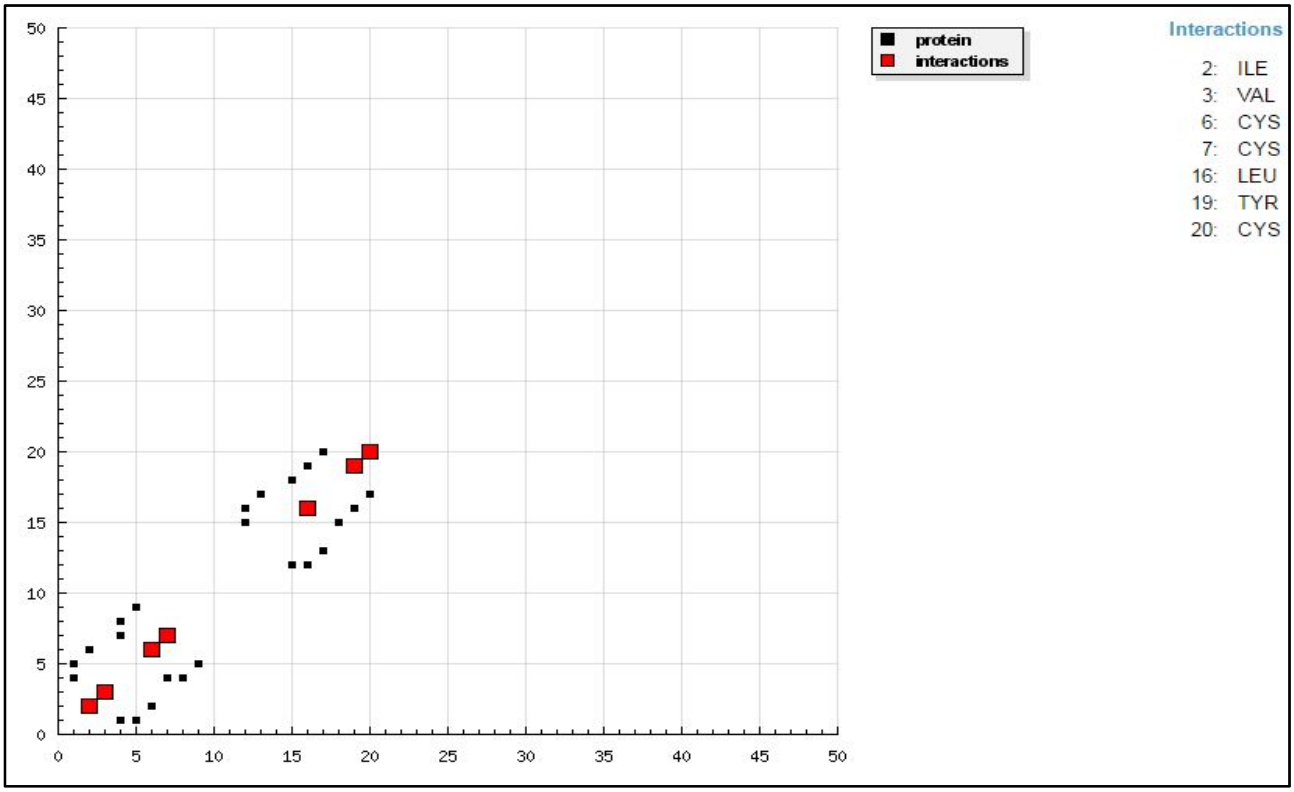

Fig. 9 HB bends of interface among BOD composite with receptor of breast cancer mutant 3tt8.

values, when available, and the Gibbs free energy is negative [53-55]. Also, based on this data, it can propose that interaction between the 3tt8 receptor and the BOD composite is possible". 2D diagrams of docking with BOD composite are revealed in Fig. 10.

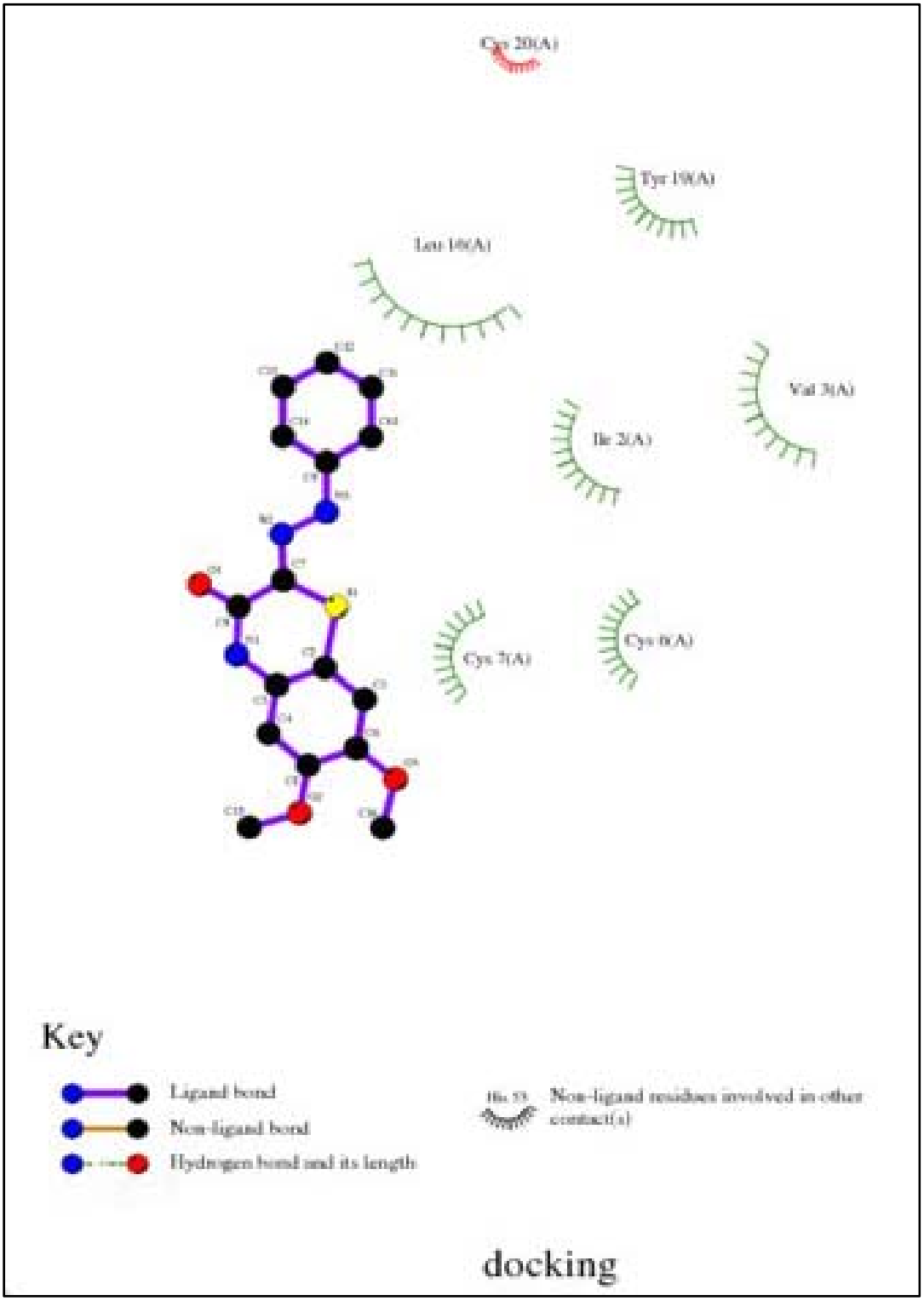

Fig. 10 2D bends of interface among BOD composite with 3tt8 receptor.

3.8. Mechanism of Corrosion Protection

From the electrochemical tests the IE % count on dose, nature of metal, surface conditions and the kind of adsorbed inhibitor on P355 Cs.

The outcome data of corrosion data presence of this inhibitor:

1. The minor of CR with increase in dose of the inhibitor.
2. The exchange in Tafel lines to higher regions of potential.
3. The %*IE* is dependent on charge density and their apparatus of adsorption centers in the BOD.

It was detected that the kind of adsorption relies on the affinity of P355 Cs and the against clouds of π-electron of the ring. Metals such as iron, which has a higher attract against aromatic moieties, was gotten to adsorb benzene rings in orientation flat.

BOD composite exhibits excellent inhibition power due to: (i) the existence of two methyl groups which are an electron donating groups, also these groups will improve the electron charge density on the molecule, (ii) its greater molecular size (264.32) that may facilitate excellent surface coverage, and (iii) its adsorption through three active centers (1 − O and 2 − N atoms).

4. Conclusions

1. BOD is excellent corrosion inhibitor for P355 Cs in 1.0 N corrosive solution.
2. C_{dl} lower with respect to blank solution when the added BOD inhibitor. This fact may suggested by inhibitor BOD molecule adsorbed of the on the P355 Cs surface.
3. Molecular docking and binding energy measurements of BOD composite with the receptor of 3tt8 − hormone of crystal structure analysis of Cu Human Insulin Derivative indicated that the composite is efficient inhibitor of receptor of 3tt8 − hormone.
4. The morphology of protected and unprotected P355 Cs was examined by SEM and EDX.
5. Quantum chemistry measurement results showed that the heteroatoms of N and O are the active sites of the BOD compound. It can absorb on Fe surface firmly by donating electrons to Fe atoms and accepting electrons from 3d orbital of Fe atoms.

References

[1] Shahryari, A., Omanovic, S., Fan, B. M. 2018. "Understanding the Inhibition Mechanism of a Supramolecular Complex as the Corrosion Inhibitor for Mild Steel in the Condensate Water." *J. Materials Science Forum* 913: 424-38.

[2] Luo, H., Su, H., Dong, C., and Li, X. 2017. "Passivation and Electrochemical Behavior of 316L Stainless Steel in Chlorinated Simulated Concrete Pore Solution." *J. Appl. Surf. Sci.* 400: 38-48.

[3] Luo, H., Dong, C., and Xiao, K. 2017. "Passive Film Properties and Electrochemical Behavior of Co-Cr-Mo Stainless Steel in Chloride Solution." *J. Materials Engineering and Performance* 26: 2237-43.

[4] Olivio, P. H. P., and Correia, L. A. 2018. "Exploring Electrochemical Reactivity toward Ametryn of Hybrid Silicate Films with Phosphomolybdic Acid." *J. Materials Science and Engineering: B.* 229: 13-9.

[5] Shahryari, A., Omanovic, S., and Szpunar., J. A. 2016. "Enhancement of biocompatibility of 316LVM Stainless Steel by Cyclic Potentiodynamic Passivation." *J. Biomedical Materials Research* 676: 414-23.

[6] Wan, H., Song, D., Zhang, D., and Du., C. 2018. "Corrosion Effect of Bacillus Cereus on X80 Pipeline Steel in a Beijing Soil Environment." *J. Bioelectrochemistry* 121: 18-26.

[7] Zhang, S., Jiang, Z., and Zhang, B. 2017. "Detection of Susceptibility to Intergranular Corrosion of Aged Super Austenitic Stainless Steel S32654 by a Modified Electrochemical Potentiokinetic Reactivation Method." *J. Alloys and Compounds* 695: 3083-93.

[8] Juan, L., Rong, G., Lan, G., and Liy, F. 2016. "Mechanical characterization of Waste-Rubber-Modified Recycled-Aggregate Concrete." *J. Cleaner Production* 124: 325-38.

[9] Liu, C. 2007. "Corrosion Resistance of Titanium Ion Implanted AZ91 Magnesium Alloy." *J. Vacuum Science & Technology A: Vacuum, Surfaces and Films* 25: 334-45.

[10] Fan, L., Tang, F., and Singo, T. 2017. "Corrosion Resistances of Steel Pipes Internally Coated with Enamel." *J. Corrosion* 73: 1335-45.

[11] Tavares, S. S. M., Pardal, J. M., and Pardal, J. P. 2016. "Investigation of the Failure in a Pipe of Produced Water

from an Oil Separator due to Internal Localized Corrosion." *J. Engineering Failure Analysis* 61: 100-7.

[12] S. M., Abd El Haleem, Abd, S., and Bahgat, A. 2013. "Environmental Factors Affecting the Corrosion Behaviour of Reinforcing Steel. V. Role of Chloride and Sulphate Ions in the Corrosion of Reinforcing Steel in Saturated $Ca(OH)_2$ Solutions." *J. Corros. Sci.* 75: 1-17.

[13] Videm, K., and Kavrekval, J. 1995. "Corrosion of Cs in Carbon Dioxide-Saturated Solutions Containing Small Amounts of Hydrogen Sulfide." *J. Corrosion* 52 (4): 260-9.

[14] Pan, Y., Dong, C., and Xiao, K. 2018. "In-situ Investigation of the Semiconductive Properties and Protective Role of Cu_2O Layer Formed on Copper in a Borate Buffer Solution." *J. Electroanalytical Chemistry* 809: 52-8.

[15] Arjmand, F., and Zhang, L. 2015. "Electrochemical Corrosion Performance of Mechanically Polished Alloy 690TT at High-Temperature Water (200°C)." *J. Corrosion* 71: 1481-14898.

[16] Xun, W., Lulu, L., and Hui, L. 2018. "Effect of Strain Level on Corrosion of Stainless Steel Bar." *J. Construction and Building Materials* 163: 189-99.

[17] Wang, Z., Zhang, L., and Tang, X. 2017. "The Surface Characterization and Passive Behavior of Type 316L Stainless Steel in H_2S-Containing Conditions." *J. Appl. Surf. Sci.* 423: 457-64.

[18] Shangyi, S., and Zuo, Y. 2014. "The Improved Performance of Mg-rich Epoxy Primer on AZ91D Magnesium Alloy by Addition of ZnO." *J. Corrosion Science* 87: 167-78.

[19] Bensabra, H., and Azzouz, N. 2013. "Study of Rust Effect on the Corrosion Behavior of Reinforcement Steel Utilizing Impedance Spectroscopy." *J. Metallurgical and Materials Transactions A* 44: 5703-10.

[20] Zhang, P., Zhaolin, L., and Wang, Y. 2018. "3D Neutron Tomography of Steel Reinforcement Corrosion in Cement Based Composites." *J. Constr. Build. Mater.* 162: 561-5.

[21] Sung, H., Kumar, J., and Sun, W. 2017. "Effect of $LiNO_2$ Inhibitor on Corrosion Characteristics of Steel Rebar in Saturated $Ca(OH)_2$ Solution Containing NaCl: An Electrochemical Study." *J. Constr. Build. Mater.* 133: 387-96.

[22] Ming, J., Jinjie, S., and Sun, W. 2018. "Effect of Mill Scale on the Long-Term Corrosion Resistance of a Low Alloy Reinforcing Steel in Concrete Subjected to Chloride Solution." *J. Constr. Build. Mater.* 163: 508-5176.

[23] Casini, J., Saeki, M., and Takiishi, H. 2017. "Effect of Sn and Cu on Corrosion Resistance of La Mg Al Mn Co Ni Type Alloys." *J. Materials Science Forum* 889: 353-7.

[24] Eldesoky, A. M., El-Bindary, M. A., El-Sonbati, A. Z., and Morgan, Sh. M. 2015. "New Eco-Friendly Corrosion Inhibitors based on Azo Rhodanine Derivatives for Protection Copper Corrosion." *J. Mater. Environ. Sci.* 6: 2260-76.

[25] Eldesoky, A. M., Diab, M. A., El-Bindary, A. A., El-Sonbati, A. Z., and Seyam, H. A. 2015. "Some Antipyrine Derivatives as Corrosion Inhibitors for Copper in Acidic Medium: Experimental and Quantum Chemical Molecular Dynamics Approach." *J. Mater. Environ. Sci.* 6: 2148-65.

[26] Shoair, A. F., El-Bindary, A. A., El-Sonbati, A. Z., and Beshry, N. M. 2016. "Molecular Docking, Potentiometric and Thermodynamic Studies of Some Azo Quinoline." *J. Molecular Liquids* 215: 740-8.

[27] Halgren, T. A. 1996. "Merck Molecular Force Field. I. Basis, Form, Scope, Parameterization, and Performance of MMFF94." *J. Comput. Chem.* 17: 490-519.

[28] Morris, G. M., and Goodsell, D. S. 1998. "Automated Docking Utilizing a Lamarckian Genetic Algorithm and an Empirical Binding Free Energy Function." *J. Comput. Chem.* 19 (14): 1639-62.

[29] Sharma, N. K., Jha, K. K., and Vijaya Kumar, M. 2014. "Synthesis and Antimicrobial Evaluation of 2-(2-(Benzo [d] Oxazol-2-yl) Phenylamino)-n-(Substituted Phenyl) Acetamides." *J. Pharmaceutical Science and Research* 5 (8): 3260-6.

[30] Al-Khaldi, M. A., and Al-qahtani, K. Y. 2013. "Corrosion Inhibition of Steel by Coriander Extracts in Hydrochloric Acid Solution." *J. Mater. Environ. Sci.* 4 (5): 593-600.

[31] Khaled, K. F. 2008. "Adsorption and Inhibitive Properties of a New Synthesized Guanidine Derivative on Corrosion of Copper in 0.5 M H_2SO_4." *J. Applied Surface Science* 255(5): 1811-8.

[32] Rios, J. F., Calderon, J. A., and Nogueira, R. P. 2013. "Electrochemical Behavior of Metals Utilizied in Drinking Water Distribution Systems: A Rotating Cylinder Electrode's Study." *J. Corrosion* 69 (9): 875-85.

[33] Macdonald, D. D., and Mckubre, M. C. H. 1982. "Impedance Measurements in Electrochemical Systems." *Modern Aspects of Electrochemistry*, edited by Bockris, J. O'M., Conway, B. E., and White, R. E.: Plenum Press, New York 14: 61-150.

[34] Carbonini, P., Monetta, T., and Scatteia, B. 1979. "Degradation Behaviour of 6013-T6, 2024-T3 Alloys and Pure Aluminium in Different Aqueous Media." *J. Applied Electrochemistry* 27: 1135-43.

[35] Gabrielli, C. 1984. "Identification of Electrochemical Processes by Frequency Response Analysis." *Solarton Instrumentation Group*, 2-15.

[36] Sun, Y. M., and Chen, H. L. 2012. "Electrochemical Measurements of Corrosion Inhibition of Mild Steel in Sulfuric Acid by BIMGCS12-3." *J. Advanced Materials Research* 402: 800-3.

[37] Anejjar, A., Zarrouk, A., Salghi, R., Zarrok, H., Ben Hmamou, D., Hammouti, B., Elmahi, B., and Al-Deyab, S. S. 2013. "Studies on the Inhibitive Effect of the Ammonium Iron (II) Sulphate on the Corrosion of Cs in HCl Solution." *J. Mater. Environ. Sci.* 4 (5): 583-92.

[38] Mertens, S. F., Xhoffer, C., Decooman, B. C., and Temmerman, E. 1997. "Short-Term Deterioration of Polymer-Coated 55% Al-Zn Part 1: Behavior of Thin Polymer Films." *J. Corrosion* 53: 331-88.

[39] Murthy, H. C. 2015. "Electroanalytical Study on the Corrosion Behaviour of TiO_2 Particulate Reinforced Al 6061 Composites." *J. Material Science Research India* 12 (2): 112-26.

[40] Fouda, A. S., Ibrahim, H., and Atef, M. 2017. "Adsorption and Inhibitive Properties of Sildenafil (Viagra) for Zinc in Hydrochloric Acid Solution." *J. Results in Physics* 7: 3408-18.

[41] Abdulwahed, J. A. M., Younis, R. M., Hassan, H. M., Elsayad, M. R., and Eldesoky, A. M. 2016. "Electrochemical and Surface Characterization Studies on C38 Steel in 1 M Hydrochloric Acid Medium Utilizing Prop-2-en-1-one Derivatives as Corrosion Inhibitors." *Int. J. Adv. Res.* 4 (11): 1192-203.

[42] Lagrenée, M., Mernari, B., Bouanis, M., Traisnel, and M., Bentiss, F. 2002. "Study of the Mechanism and Inhibiting Efficiency of 3,5-bis(4-methylthiophenyl)-4H-1,2,4-triazole on Mild Steel Corrosion in Acidic Media." *J. Corros. Sci.* 44: 573-88.

[43] McCafferty, E. 2005. "Validation of Corrosion Rates Measured by the Tafel Extrapolation Method." *J. Corros. Sci.* 47 (12): 3202-15.

[44] Zhang, S. S., Xu, K., and Jow, T. R. 2003. "The Low Temperature Performance of Li-ion Batteries." *J. Power Sources* 115 (1): 137-40.

[45] Rauf, A., Bogaertsd, W. F., and Mahdi, E. 2012. "Implementation of Electrochemical Frequency Modulation to Analyze Stress Corrosion Cracking." *J. Corrosion* 68 (3): 1-9.

[46] Fouda, A. S., and Abdulwhed, H. A. 2016. "Corrosion Inhibition of Copper in HNO_3 Solution Utilizing Thiophene and its Derivatives." *Arabian, J. of Chemistry* 9: 519-99.

[47] Samie, F., and Tidblad J. 2008. "Influence of Nitric Acid on Atmospheric Corrosion of Copper, Zinc and Css." *J. Corrosion Engineering, Science and Technology* 43 (2): 117-22.

[48] Javadian, S., Yousefi, A., and Neshati, J. 2013. "Synergistic Effect of Mixed Cationic and Anionic Surfactants on the Corrosion Inhibitor Behavior of Mild Steel in 3.5% NaCl." *J. Applied Surface Science* 285: 674-81.

[49] Jafari, H., and Sayin, K. 2016. "Sulfur Containing Composites as Corrosion Inhibitors for Mild Steel in Hydrochloric Acid Solution." *J. Transactions of the Indian Institute of Metals* 69 (3): 805-15.

[50] Han, W., Pan, C., Wang, Z., and Guocai, Y. 2015. "Initial Atmospheric Corrosion of Cs in Industrial Environment." *J. Materials Engineering and Performance* 24 (2): 864-74.

[51] Lukovits, I., Palfi, K., Bako, I., and Kalman, E. 1997. "LKP Model of the Inhibition Mechanism of Thiourea Composites." *J. Corrosion* 53 (12): 915-9.

[52] Zhang, S., and Zhihua, T. 2009. "The Effect of Some Triazole Derivatives as Inhibitors for the Corrosion of Mild Steel in 1.0 N Corrosive Solution." *J. Appl. Surf. Sci.* 255 (15): 6757-63.

[53] Morgan, Sh. M., and Refaat, H. M. 2016. "Molecular Docking, Geometrical Structure, Potentiometric and Thermodynamic Studies of Moxifloxacin and its Metal Complexes." *J. Mol. Liq.* 220: 802-12.

[54] Sayin, K., and Karakas, D. 2018. "Computational Investigations of Trans-Platinum(II) Oxime Complexes Utilizied as Anticancer Drug." *J. Spectrochimica Acta Part A: Molecular and Biomolecular Spectroscopy* 188: 537-46.

[55] El-Bindary, A. A., El-Sonbati, A. Z., and Diab, M. A. 2016. "Molecular Docking, Potentiometric and Thermodynamic Studies of Some Azo Composites." *J. Solution Chemistry* 45 (7): 990-1008.